

A novel method of measuring upwelling radiance in the hydrographic sub-hull

N. Rüssmeier

nick.ruessmeier@uni-oldenburg.de

O. Zielinski

oliver.zielinski@uni-oldenburg.de

Institute for Chemistry and Biology of the Marine Environment, University of Oldenburg,
26111 Oldenburg, Germany

Institute for Chemistry and Biology of the Marine Environment, University of Oldenburg,
26111 Oldenburg, Germany

In this study we present a new method useful in collecting upwelling radiance (L_u) from a platform submerged in a hydrographic sub-hull or moon pool of a research vessel. The information analyzed here was obtained during a field campaign in the Northwestern European shelf seas aboard the new research vessel SONNE. As the platform was located at the center of the ship, there is minimal effect from pitch and roll which is known to influence upwelling radiance observations. A comparison of the measurements from this platform with a free falling hyperspectral profiler was performed to determine the degree of uncertainty that results from ship shadow. For given $L_u(\lambda)$ in situ data we observed $\pm 33\%$ intensity deviations compared to profiling measurements that can be attributed to instrument shading during moon pool installation and environmental perturbations. Furthermore $L_u(\lambda)$ in situ spectra variations were observed at lower wavelengths, therefore a form fitting algorithm was adapted to receive corresponding depths with identical spectral form from $L_u(z, \lambda)$ profiler casts. During an east to west transect in North Sea with a schedule speed up to 12 knots in situ radiance reflectance $r_{rs}(z, \lambda)$ measurements at 7 meter depth were performed with this novel radiometer setup. In spite of any restrictions originating from the sub-hull installation, water masses mixing zone from CDOM dominated coastal waters in the Skagerrak Strait towards the open North Sea were successfully derived thus offering an underway applicable upwelling radiance sensing not suffering from sun glint or other typical restrictions of above water radiometer installations.

[DOI: <http://dx.doi.org/10.2971/jeos.2016.16003>]

Keywords: Shipborne remote sensing, underway, ocean color, hyperspectral sensing, shadow, RV SONNE

1 INTRODUCTION

Understanding how light interacts with optically active constituents of natural waters has improved in the last few years due to smaller, fast, unmanned, automate and affordable optical tools and improved bio-optical models [1]–[3]. These optical tools can be mounted on fixed or mobile platforms allowing measurements to be collected continuously at sea in either a horizontal or vertical profile [4]–[6]. However, in the ocean color community remote sensing of apparent optical properties with minimal uncertainties is either done using above water installations or in situ observations with profiling equipment at selected stations [4, 7, 8]. Most observations are dependent on available sunlight, wind speed influencing surface reflected glint, instrument or platform shading, optical sensor accuracy, sensitivity, spatial and spectral resolution. These factors therefore determine processes in the ocean we can understand especially in the time and space domain [1, 9, 10].

Deriving information about the ocean from measured reflected sunlight using submerged optical sensors offers a reasonable method that is less susceptible to sea surface conditions resulting in a low signal to noise ratio influenced by surface reflected glint. One alternative is a dome covered radiometer mounted on drift stabilized buoy just below the air-sea surface level [11]. In this study we present a new method of collecting upwelling radiance underway in the ship's hull

of the German research vessel RV SONNE at 7 m depth, near to the center of the vessel. The presented method offers the capability to obtain near real-time hyperspectral in situ data underway. The sampling setup is relatively robust and requires less effort with respects to post processing and instrument setup requirements compared to above water shipborne remote sensing or free falling profiling tools. Furthermore, free falling profilers tend to suffer from tilt problems in the upper ocean resulting from turbulence and therefore might not provide accurate or valuable information about light in the near sea surface waters [12]. The goal here was to present a novel setup, measurements that were obtained in situ, evaluate possible source of error and quantify them. A comparison of the measurements from this new setup was made with a hyperspectral free falling profiler. As the main challenge of the setup is ship shading [13]–[15] we also propose possible methods to mitigate uncertainties hence maintaining quality and quantity of measurements.

2 METHODS AND MATERIALS

2.1 Sampling

Underway measurements of upwelling radiance $L_u(0^-, \lambda)$, downwelling cosine irradiance $E_d(0^+, \lambda)$ and matching

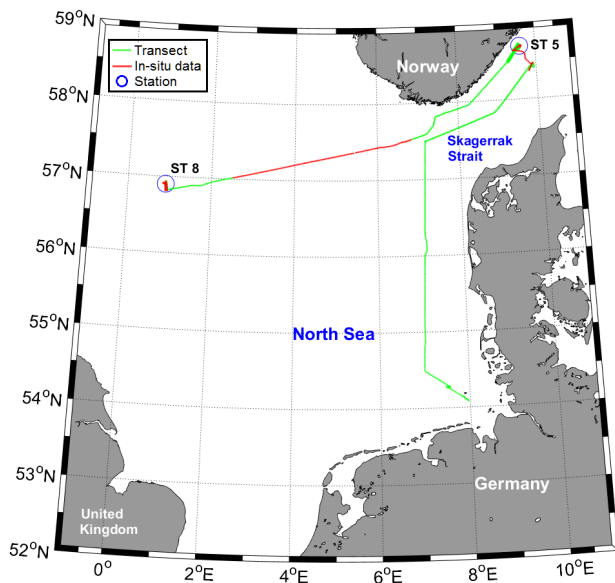


FIG. 1 Field campaign transect in the North Sea (green), availability of in situ data (red) and stations investigated in this study.

Station	Date	Time UTC	Cloud cover (%)	Sun zenith angle θ (°)
ST5	2014-27-09	12:30	20	62
ST8	2014-29-09	12:30	100	59

TABLE 1 Summary of matching in situ sampling using the profiler.

hyperspectral profiler casts were conducted aboard the RV SONNE during a field campaign between September 23 and October 1, 2014 in the North Sea. In Figure 1 the transect with indications of in situ data and stations are shown, while Table 1 summarizes the measurement conditions at station ST5 and ST8.

2.2 Measurement systems

Data from three systems (in situ installation, in water profiles and vessel metadata) was used to assess the radiance radiometer installation under the ship’s hull. In situ measurement under the vessel hull was realized with a calibrated RAMSES-ARC hyperspectral radiance meter (320–950 nm) (TriOS, Germany) to measure upwelling radiance $L_u(7, \lambda)$ in 7 m depth and at 1 minute intervals. The installation was possible in a so-called “hydrographic sub-hull support” (HSHS): a comprehensive transducer support set (e.g. for hydrophones, speedometers, transmitter-receivers, video cameras) which is used to deploy an instrument in a well all the way under the hull of a ship, at a level that can be adjusted between 0 to 1 meter [16]. In this study a 0.5 meter extension has been used for the RAMSES-ARC installation (see Figure 2). Additionally a calibrated RAMSES-ACC hyperspectral radiometer located on deck measured downwelling cosine irradiance $E_d(0^+, \lambda)$ at 5 minute intervals above water surface to correct for incoming light fluctuations. The positions of the radiometers are shown in Figure 3.

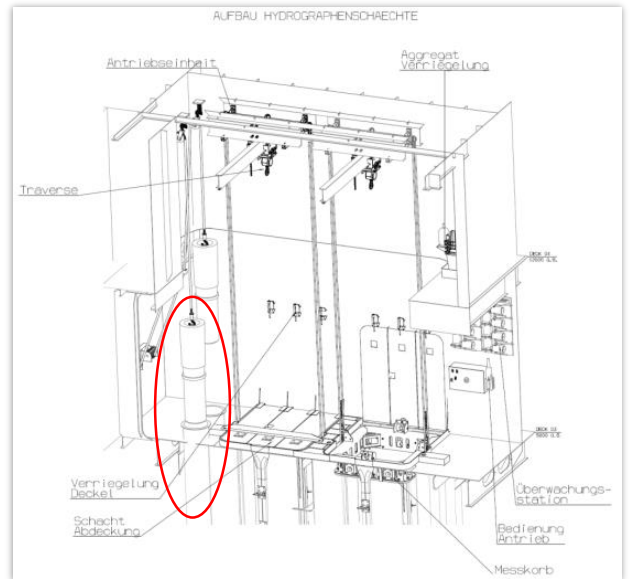
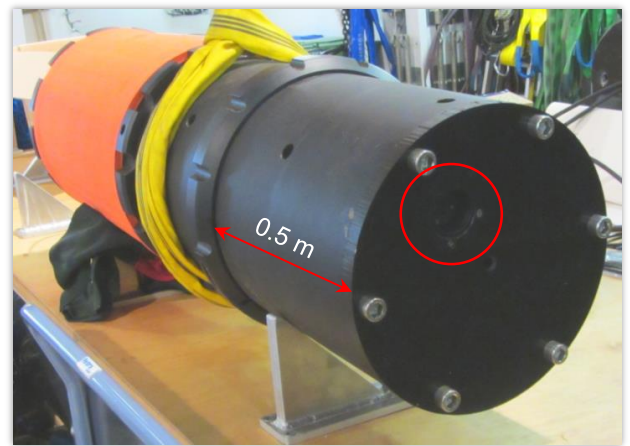


FIG. 2 Hydrographic sub-hull support with TriOS RAMSES ARC hyperspectral radiance radiometer (top), (bottom) Hydrographic funnels setup on RV SONNE.

The field of view of the RAMSES-ARC meter (approximately 7° field-of-view in air) in a depth of about 6.9 m (6.4 m draught + 0.5 m HSHS) directly under the vessel hull was influenced by the ship’s shadow and shows a diffuse light field without direct influence of wave induced light focusing or rough sea surface. The influence of the vessels pitch and roll effects on the installed instrument in the sub hull support is minimal because of the centered position in relation to the vessel dimensions.

Concurrent with $L_u(7, \lambda)$ measurements under the ship’s hull, vertical free fall profiles of upwelling radiance $L_u(z, \lambda)$ within the water column were performed at available stations (ST5, ST8) with a HyperPro II (Satlantic, Canada) equipped with an HyperOCR radiance meter (calibrated 350–800 nm). At each station three back-to-back profiles (named a, b and c) were measured approximately 50 meter abaft, performed from main deck of the research vessel to avoid shadowing influences from the ship’s superstructure. Internal tilt sensors quantified the vertical orientation of the profiler as it fell through the water. Data processing including raw data calibration and tilt angle filtering ($\pm 5^\circ$ acceptance range) were performed using the ProSoft Software version 7.7.16 (Satlantic Inc., Canada). After applying tilt filtering $L_u(z, \lambda)$, data down

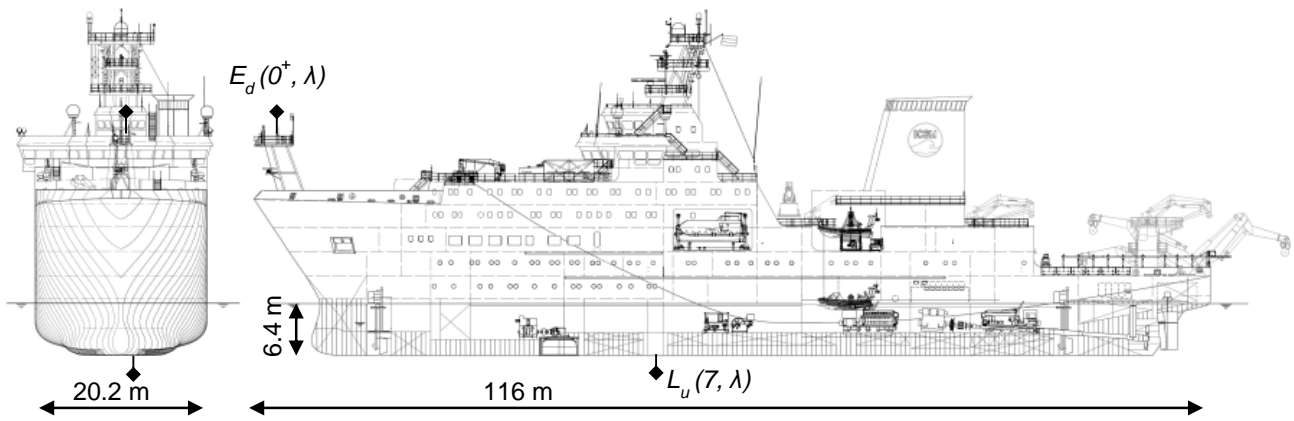


FIG. 3 Schematic of the TriOS RAMSES radiometers in situ setup on RV SONNE.

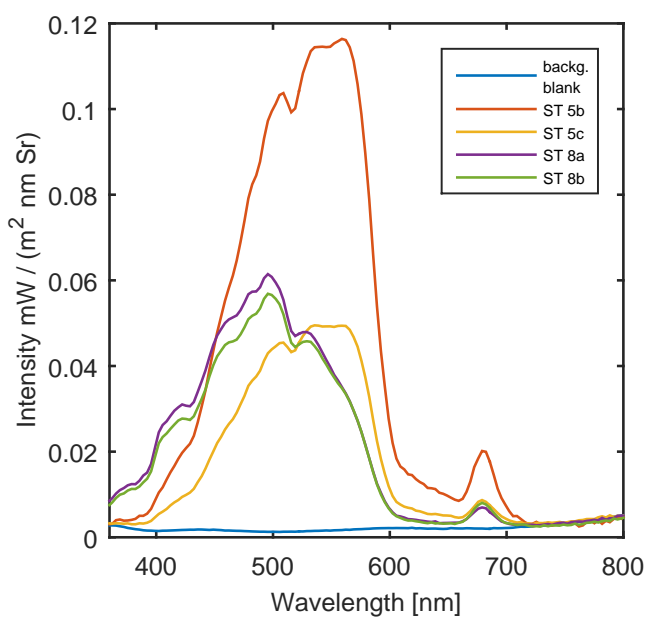


FIG. 4 Upwelling radiance spectra at 7 meter at the two stations (each with two casts available) measured via the HyperPro II, Satlantic.

to 7 meter for ST5 cast (a) and ST8 cast (c) have been removed. The upwelling radiance spectra for the remaining 4 casts at a depth of 7 meter are given in Figure 4. Furthermore the extensive metadata from DSHIP (Data Acquisition and Management System for technical, nautical and scientific data, Werum, Germany) and the station book were used to consider the influence of cloud cover (approximated from visual inspection), global radiation (Biospherical QSR-2000 with 1 minute sampling interval, sensor located centered on deck), ship's heading and position relative to the radiance measurements.

3 DATA ANALYSIS, RESULTS AND DISCUSSION

As mentioned the radiometer setup under the ship's hull is influenced from ship's superstructure shadow. Therefore in the first data analysis part we will consider the $L_u(\lambda)$ spectra from in situ and profile measurements during stations before we proceed with the second data analyses part, the

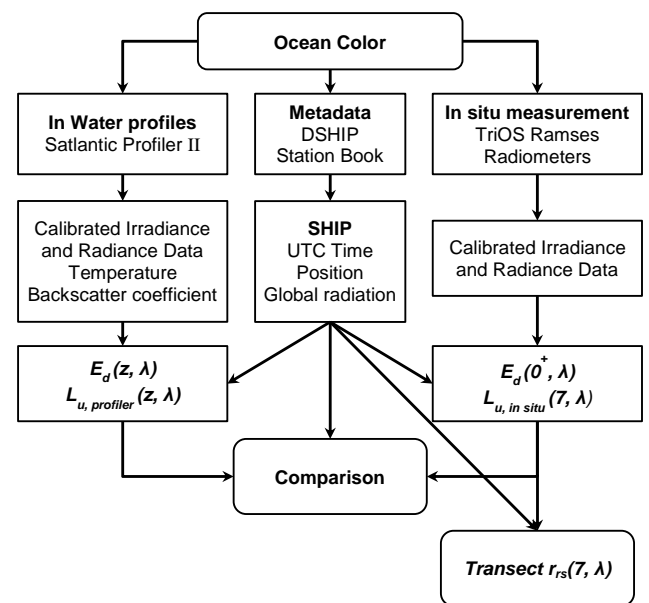


FIG. 5 Flowchart of methods and systems with respect to in water profile, in situ measurement and ship's metadata.

underway in situ measurements and interpretation of spectral radiance reflectance $r_{rs}(7, \lambda)$ during transect. This procedure should indicate to what extent the in situ installation is affected by shadowing. The flowchart of the processing is shown in Figure 5. Further studies of ship's shadow effect on in-water radiance prepared with Monte Carlo simulations from Piskozub [13] illustrate relative errors for upwelling radiance close to the ship in a range from 22% (sunny side) up to 60% (shadow side). Also Piskozub [13] shows that the sun zenith angle θ can induce up to 10% (at $\theta = 60^\circ$) relative irradiance error for shadowed instruments near the ship hull.

Sun zenith angles θ during comparative measurements at ST5 (62°) and ST8 (59°) were computed using the solar position algorithm [17]. The sea roughness at the two stations was nearly identical and showed smooth low waves without whitecaps. This provides very similar sun zenith and wave conditions at both stations. Most important differences between the two stations were the inherent optical properties, e.g. absorption and scattering coefficient as well as downwelling irradiance $E_d(0^+, \lambda)$ due to different cloud cover. During transect with

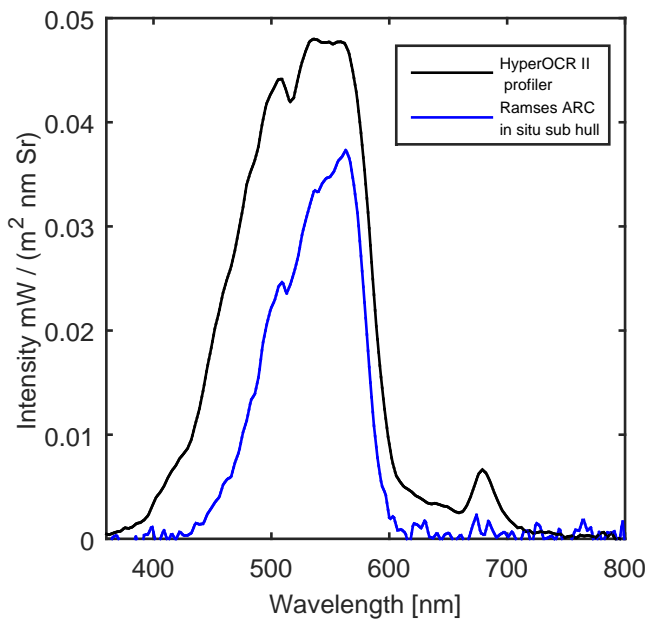


FIG. 6 Upwelling radiance from HyperPro II cast and Ramses ARC in situ sub-hull spectra at 7 meter for ST5c.

a vessel speed up to 12 knots it is generally possible that air bubbles submerged under the vessel hull influence upwelling radiance measurements, however since the hull of RV SONNE was especially designed for hydrographic and sound measurements, guiding air bubbles at the side of the hull, we assume that in the study presented this effect is minimal.

3.1 Comparative measures of upwelling radiance

Upwelling radiance $L_u(z, \lambda)$ profiler spectra at 7 meter at ST5 show generally a maximum around 555 nm caused by the colored dissolved organic matter (CDOM) absorption from coastal water for lower wavelength, while at ST8 in open sea conditions a maximum around 490 nm occurs (Figure 4). For both stations in situ Chl-a fluorescence at 685 nm is visible. As shown in Figure 4, the calibrated HyperOCR radiometer comprise a slight background blank effect in the $L_u(z, \lambda)$ spectra, which has been corrected for the further analysis. Background blank has been computed as a median from 122 $L_u(z, \lambda)$ measurements obtained at depths z greater than 83 meter, where no significant downwelling irradiance $E_d(z, \lambda)$ were existent that can induced upwelling radiance signal.

The profiler $L_u(z, \lambda)$ spectra at 7 meter in Figure 4 also show a strong intensity variability between ST5b and ST5c casts due to incoming light fluctuations. A comparison of the $L_u(\lambda)$ spectra (here for ST5 c) at 7 meter from the Ramses ARC in situ sub-hull installation and the HyperPro II profiler (Figure 6) show a difference in intensity and form of the spectra. The upwelling radiance intensity, mostly affected from incoming light $E_d(0^+, \lambda)$ ship shadowing as well as spectral form deviation, the latter depending on inherent optical properties (IOPs) and ship shadowing, will be studied in the following. We assumed that the incoming light $E_d(0^+, \lambda)$ and IOPs at each different station and each cast in approximately 110 meter horizontal distance are comparable for the different mea-

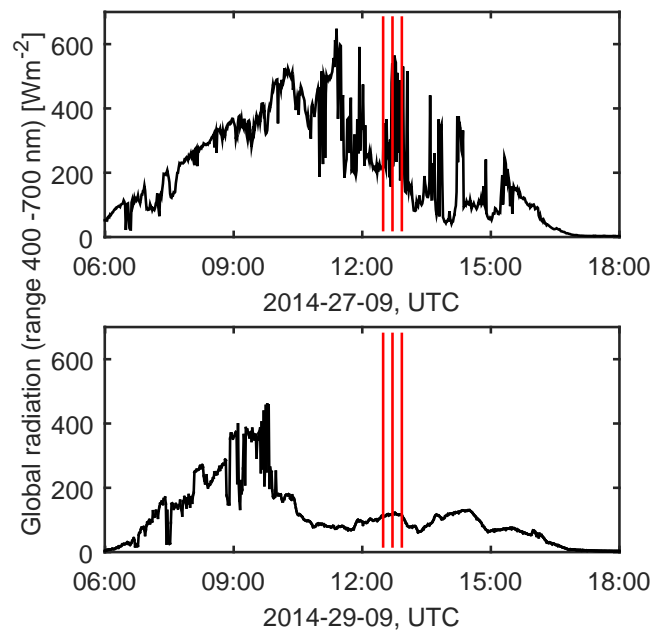


FIG. 7 Global radiation (range 400-700 nm), incoming light conditions during profiling casts a, b, c (red lines) ST5 (Top) and ST8 (Bottom) from the QSR-2000 (Biospherical, USA).

suring sites (in situ sub-hull centered 60 m to ship stern + profiler 50 m abaft ship's stern). In general each profiling measurement at station takes about 3–4 minutes and the complete three back-to-back profiles were completed within 20 minutes. Sun zenith angles θ differ therefore from beginning to ending in a range of 0.99° for ST5 and 0.64° for ST8 and therefore have no significant influence of the upwelling radiance measurement during each station. Meanwhile with a sampling interval of 1 minute corresponding sub-hull in situ $L_u(7, \lambda)$ data were obtained. In a further calculation step the average of two to four corresponding in situ sub-hull $L_u(7, \lambda)$ measurements per cast, depending on signal variation $<15\%$, were used for comparison between $L_u(7, \lambda)$ in situ sub-hull and $L_u(z, \lambda)$ profiler data.

Intensity of $L_u(7, 555 \text{ nm})$ in situ sub-hull measurements for ST5 casts with 20% cloud cover indicate lower intensity of -156% for cast (b) and -33% for cast (c) compared to profiler $L_u(z, 555 \text{ nm})$ at 7 m. Investigating the light conditions from DSHIP global radiation sensor with 1 minute sampling interval during the casts shows stronger incoming light fluctuations during ST5 (see Figure 7) while conditions for ST8 with 100% cloud cover exhibit stable incoming radiation.

In the latter case a higher intensity of $L_u(7, 490 \text{ nm})$ in situ sub-hull data was observed and yields a deviation of $+10\%$ for cast (a) and $+30\%$ for cast (b) compared to profiler $L_u(z, 490 \text{ nm})$ data at 7 m. A higher intensity of in situ sub-hull upwelling radiance signals under diffuse light conditions with ship shadow against the free falling profiler signals could originate from the reflectance effect from the ship's hull [15, 18, 19]. It can be speculated that intensity deviance at ST8 depends also to an extent in this case on local backscattering conditions from the deeper water column (see Figure 8 backscatter coefficient b_{bp}).

In addition for both stations spectral form variations in

$L_u(7, \lambda)$ for in situ sub-hull versus profiler measurements are prominent in the red to green wavelengths up to 550 nm. This wavelength dependent shading error has been also observed in studies by Weir et al. [18] and Leathers et al. [20]. Absorption in lower wavelength band can also indicate that the light path increases through the water column towards the field of view of the Ramses ARC radiometer under the ship's hull versus the light path of the HyperPro II profiler for identical IOPs and sun zenith angle θ (Figure 9).

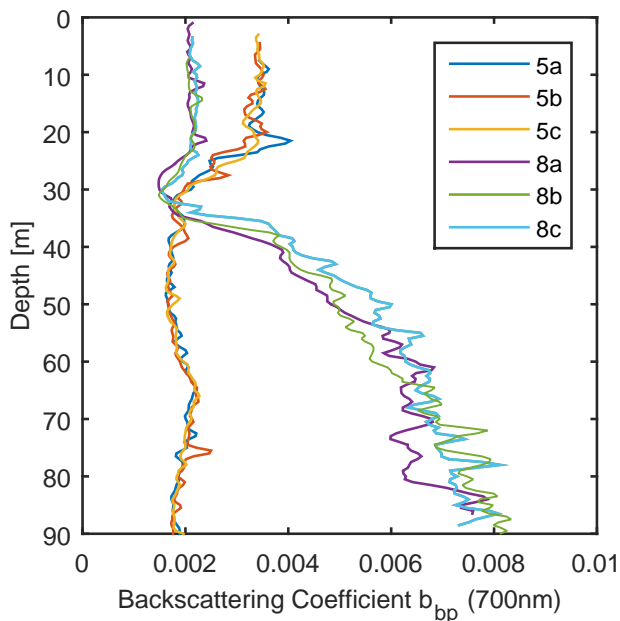


FIG. 8 Vertical profile of backscatter coefficient b_{bp} at 700 nm at ST5 and ST8.

In the following we apply a spectral fit algorithm to identify $L_u(7, 400 - 600 \text{ nm})$ in situ sub-hull spectra similar to corresponding profiler casts $L_u(z, 400 - 600 \text{ nm})$ spectra for a depth z down to 30 meter. In that range vertical profiles from the HyperPro II profiler show homogeneous physical and optical properties in both water masses at ST5 and ST8. As illustrated in Figure 10, the water temperature was nearly constant for both profiling stations up to the first 30 meter. And also the vertical profile of the backscatter coefficient b_{bp} at 700 nm at ST5 and ST8 presented in Figure 8 show for the first 30 meter similar conditions at each station. Below that temperature and backscatter signal vary in a wide range and therefore the negligible impact of physical and optical properties can not be assumed anymore. Proximity to the coast is visible at ST5 as seen from increased temperature and backscatter (at the top layer) in the Skagerrak Strait compared to ST8 open sea conditions.

A form fit depth ffd was identified as the depth where minimal spectra deviation is exhibited (matched spectral forms), assuming to what extent the ship's superstructure induced shadow affected the in situ sub-hull upwelling radiance light path versus the direct, shadow independent, profiler light path. Processing of spectral fit algorithm was performed with interpolated L_u data to full nm wavelengths. The following algorithm consists of linear normalizing the averaged TriOS in situ $L_u(7 \text{ m}, 400 - 600 \text{ nm})$ spectra and the Satlantic $L_u(z, 400 - 600 \text{ nm})$ spectra per cast to the maximum, (ST5 (563 nm) and ST8 (500 nm)) according to Eq. (1), and calculation of the spectral deviation between corresponding in situ sub-hull and profiler cast wavelengths per depth z (spectral deviation as presented in Figure 11). The spectra form fit

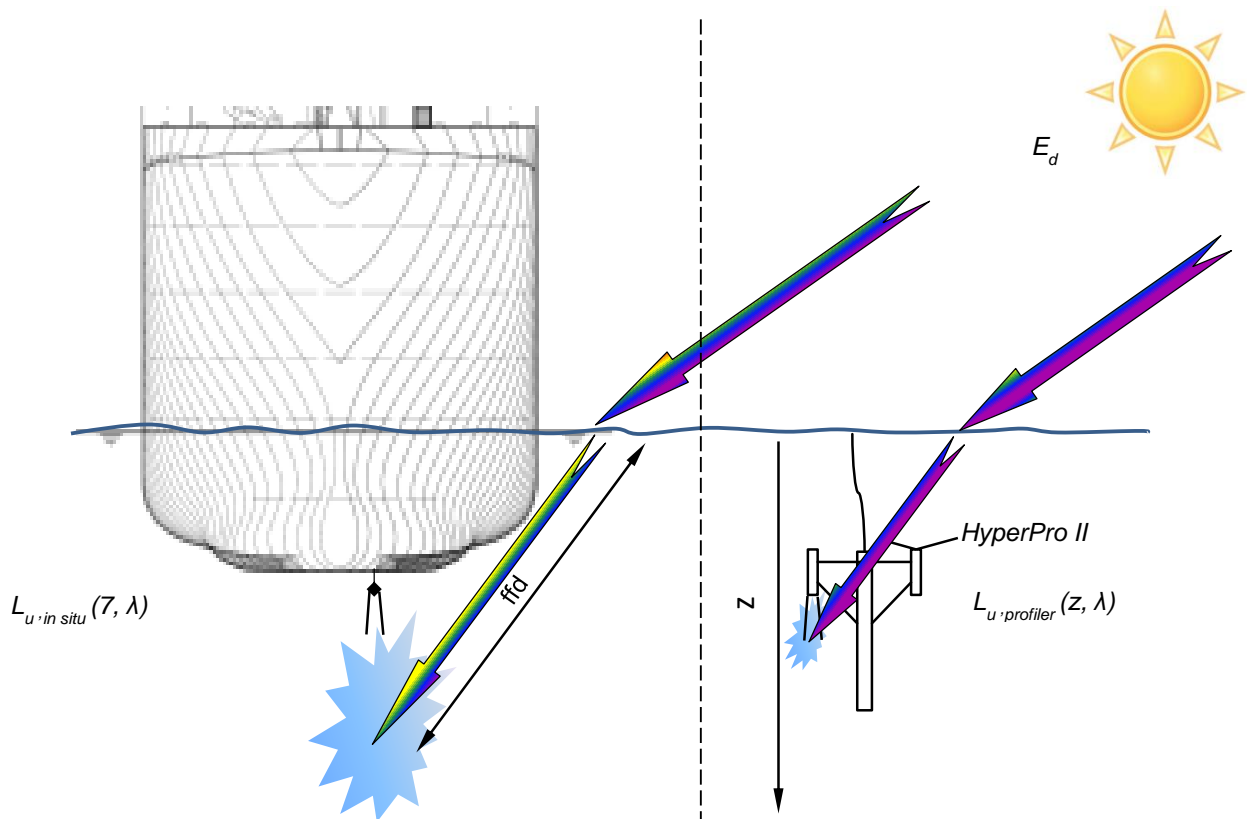


FIG. 9 Schematic light path to Ramses ARC radiometer with superstructure of RV SONNE and HyperPro II, Satlantic performing comparative measurements at station.

depth received for the minimum sum of all wavelength deviations over depths is then calculated with Eq. (2).

$$L_{U_{norm}}(\lambda) = \frac{L_U(\lambda) - \min}{\max - \min} \quad (1)$$

$$ffd = \min_{0 \rightarrow 30 \text{ m}} \sum_{400 \text{ nm}}^{600 \text{ nm}} L_{U_{norm.insitu}}(\lambda) - L_{U_{norm.cast}}(\lambda) \quad (2)$$

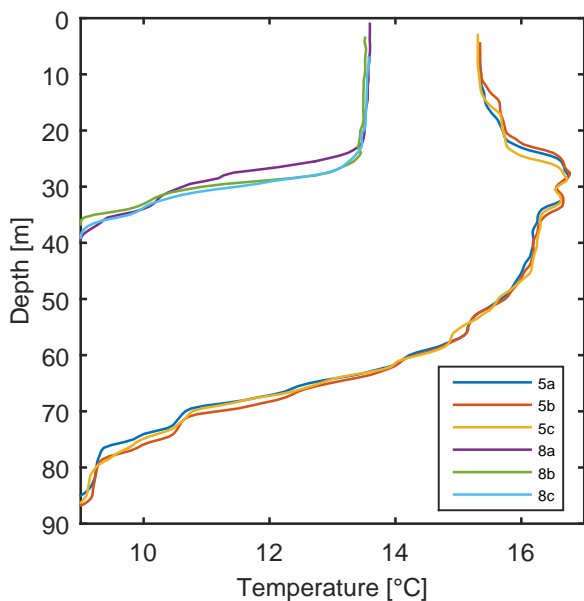


FIG. 10 Vertical temperature profiles at ST5 and ST8.

Form fitting depth results indicate a range of 17.5 m to 23.0 m for all comparisons, as presented in Table 2. Furthermore spectra deviation plots (Figure 11) show for diffuse light conditions at ST8 a better approximation and therefore less wavelength depending shadowing error than for ST5 under divergent light conditions. These results show that the upwelling radiance spectral form of the in situ installation at form fit depths are most closely corresponding to the HyperOCR upwelling radiance spectra form from the measurement of the profiler, the latter assumed to be not affected by the ship's superstructure shadow during sampling 50 m abaft ship's stern.

Furthermore the graphs in Figure 11 illustrate that ocean sampling with a free falling profiler of the upper sea surface is a tough matter due to the turbulent water body conditions induced by waves and wind. Mostly for the first 5 meters, measured data is out of the acceptance tilt angle $\pm 5^\circ$ range after filtering, even with smooth low waves which were presence during the casts at stations.

Station/cast	5a	5b	5c	8a	8b	8c
Form fit depth (m)	22	17.5	23	21.5	20.5	21

TABLE 2 Results spectra form fit depth algorithm.

3.2 Spectral radiance reflectance $r_{rs}(\gamma, \lambda)$ during east to west transect

During the westwards transect from the Skagerrak Strait to Devils Hole (North Sea) a vessel speed of up to 12 knots was reached. In situ upwelling radiance $L_u(\gamma, \lambda)$ and downwelling irradiance above surface $E_d(0^+, \lambda)$ were obtained at

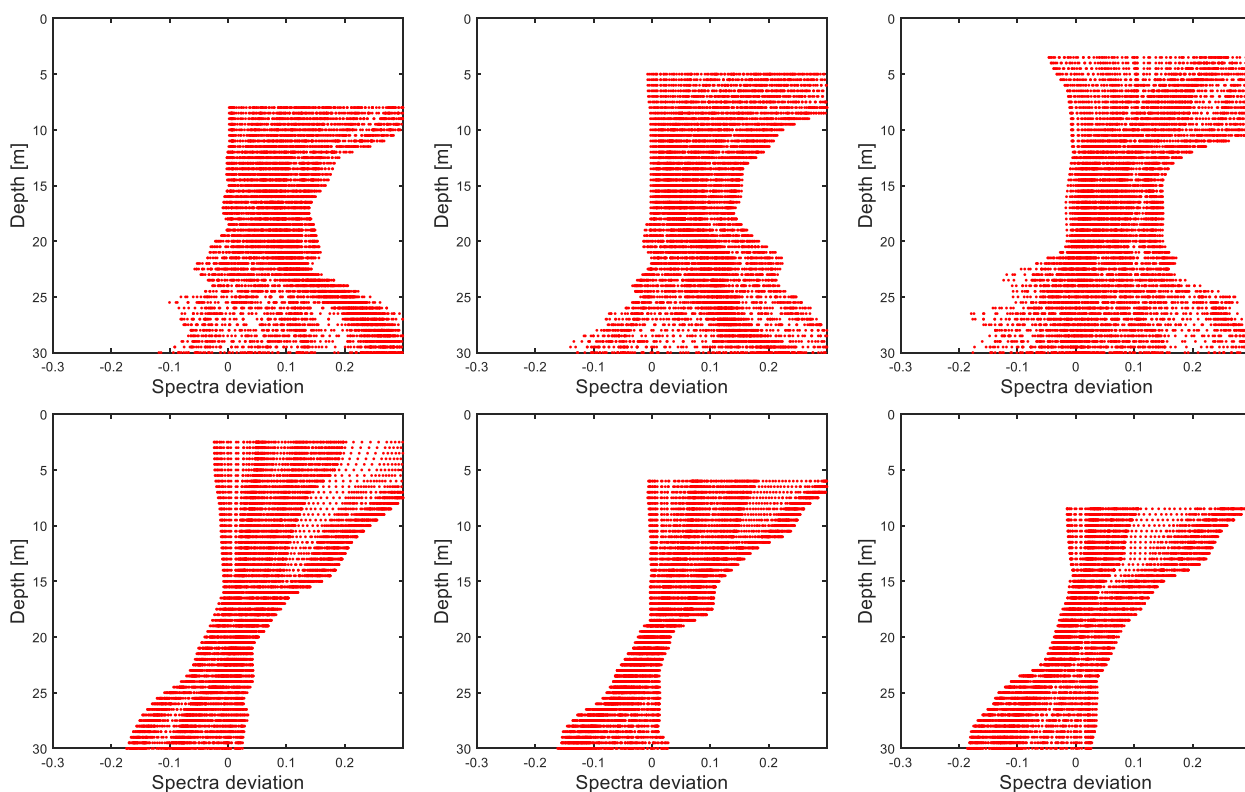


FIG. 11 Station 5 cast a, b, c (Top) and station 8 cast a, b, c (Bottom) calculated spectral wavelength deviation $L_{u,profiles}(z, \lambda)$ and $L_{u,insitu}(\gamma, \lambda)$, ($\lambda = 400-600 \text{ nm}$).

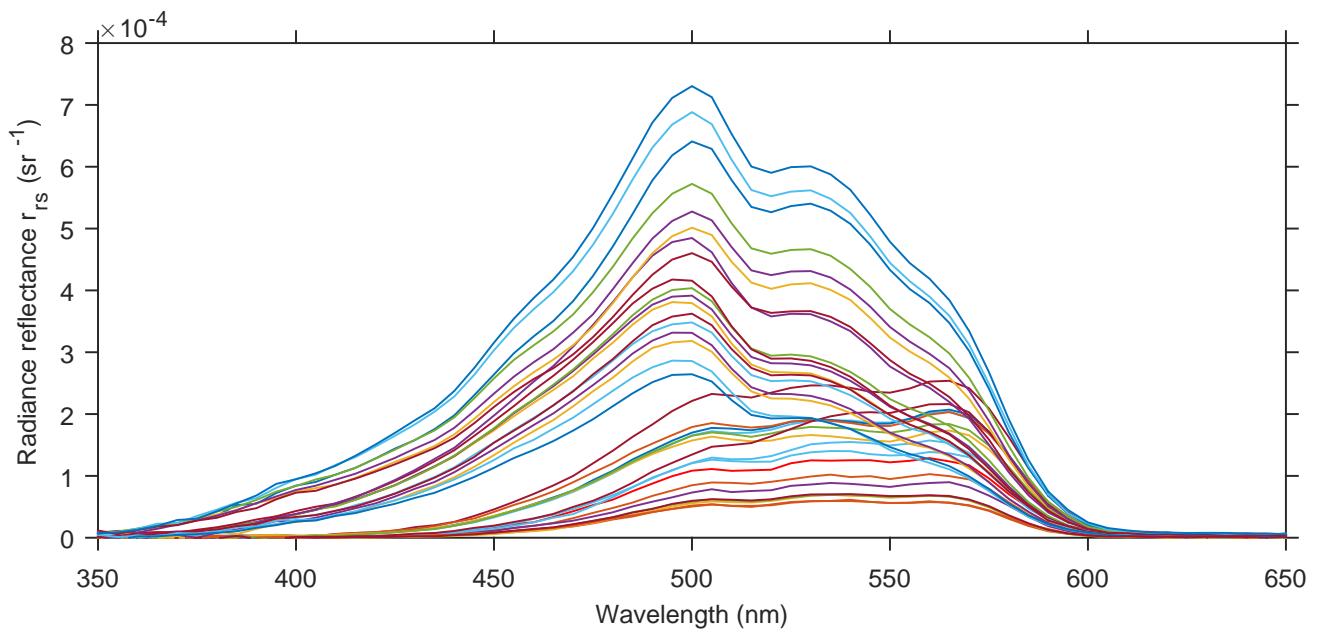


FIG. 12 Radiance reflectance spectra r_{rs} observed during transect 1014-26-09 to 1014-29-09. For reasons of clarity, only a subset of datapoints are visualized.

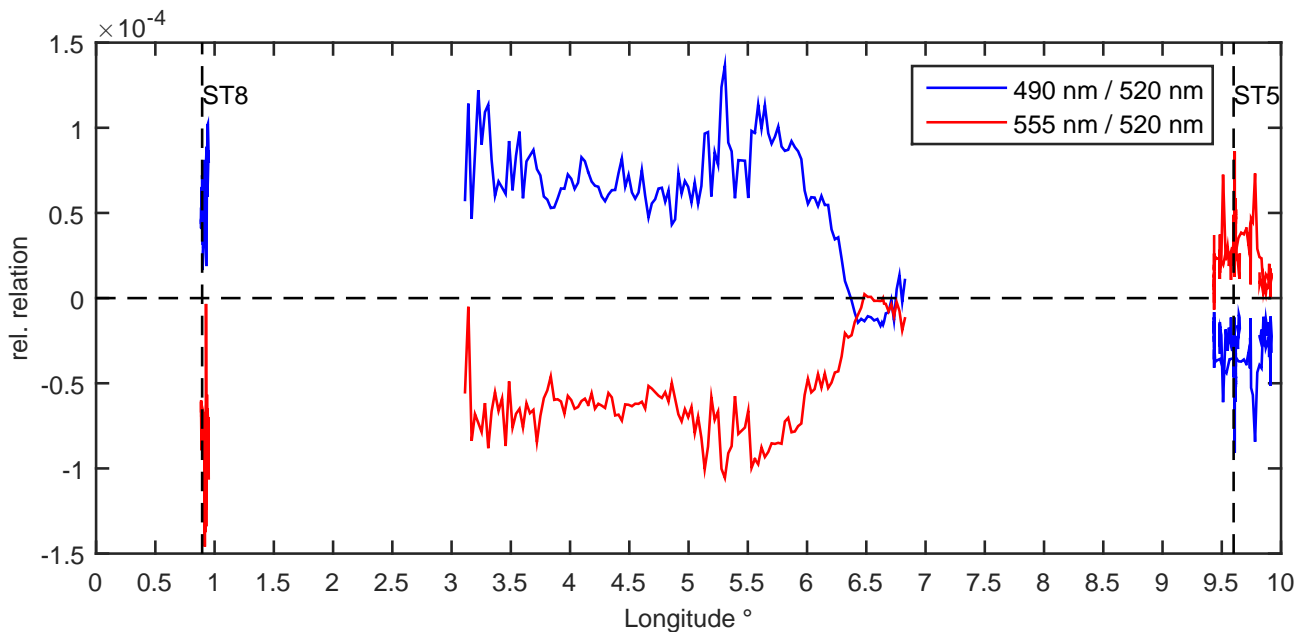


FIG. 13 Relation of 490 nm / 520 nm and 555 nm / 520 nm along the transect from 1014-27-09 to 1014-29-09.

5 minutes interval. Spectral radiance reflectance was computed as:

$$r_{rs}(7, \lambda) = \frac{L_u(7, \lambda)}{E_d(0^+, \lambda)} \quad (3)$$

Figure 12 presents a reduced dataset of 35 from origin 452 different $r_{rs}(7, \lambda)$ spectral signatures, related to the optical water characteristics.

The reduced reflectance in the blue-green region, as observed for a fraction of the spectra, is due to the absorption of colored dissolved organic matter, a suitable tracer for water mass mixing as applied by Stedmon et al. [21] and Kristiansen et al. [22] for the Baltic-North Sea. Here we investigate on the 490 nm / 520 nm and the 555 nm / 520 nm wavelength ratios to distinguish the changes of CDOM affected $r_{rs}(7, \lambda)$ spectra along the longitudinal transect during daylight (Figure 13). These wavelengths may be not related to maximum CDOM

absorption coefficient but are mostly out of the absorption range from Chl-a and regarded the ARC radiometer spectral response. Transect started at 10°E and ended westwards at 0.9°E. Around 6.7°E a reversal of the 490 nm / 555 nm relationship is visible indicating a decrease in CDOM absorption towards open North Sea water. With respect to the transect this is consistent with the 5 m depth mean surface distribution isolines of the min. CDOM absorption $a_{300 \text{ nm}}$ and $a_{375 \text{ nm}}$ in the mixing zone of North Sea and Baltic Sea water reported by [21, 22].

4 CONCLUSIONS AND OUTLOOK

We measured the upwelling radiance under the vessel hull using a new sub-hull support. The measurements were made during an east to west transect in the North Sea

while cruising with a speed of up to 12 knots. Comparison casts with a free falling profiler were performed during two available stations. The study demonstrates a practical way for underway radiance measurements during transects, providing additional support for the observation of the environmental status. Measurement of in situ sub-hull $L_u(7, \lambda)$ during ship cruise provided a cross section view over the complete east-west transect and therefore a successful way to indicate changes of interest in ocean color data as for example from Baltic Sea CDOM supply. This offers a great potential in using optical properties to trace water mass mixing, which to date has not been fully exploited by physical oceanographers. Thus the underway system, even though far from achieving the optimum of a free-from-shadow subsurface radiance measurement, can be utilized to provide a spatial context and identify locations relevant for in depth investigations. This successful application should also be seen as a motivation to use this novel particular form of sub-hull installation for additional in situ instruments (e.g. turbidity, fluorescence or oxygen sensors) enabling a closer investigation of optical-biogeochemical parameters in high resolution.

5 ACKNOWLEDGEMENTS

The authors like to thank captain and crew of RV SONNE cruise P4 for their support and also express their gratitude towards Rohan Henkel and Daniela Voß for their help with the radiometer and underway systems. The support of Shungudzemwoyo Pascal Garaba with reference contributions, discussions and constructive comments on the manuscript is gratefully acknowledged.

References

- [1] T. Platt, N. Hoepffner, V. Stuart, and C. Brown (eds.), "Why ocean colour? The societal benefits of ocean-colour technology," (IOCCG, Reports of the International Ocean-Colour Coordinating Group, No. 7, 2008).
- [2] J. Watson, and O. Zielinski (eds.), *Subsea optics and imaging* (Woodhead Publishing, Cambridge, UK, 2013).
- [3] O. Zielinski, J. A. Busch, A. D. Cembella, K. L. Daly, J. Engelbrektsson, A. K. Hannides, and H. Schmidt, "Detecting marine hazardous substances and organisms: sensors for pollutants, toxins, and pathogens," *Ocean Sci.* **5**, 329–349 (2009).
- [4] S. P. Garaba, T. H. Badewien, A. Braun, A.-C. Schulz, and O. Zielinski, "Using ocean colour remote sensing products to estimate turbidity at the Wadden Sea time series station Spiekeroog," *J. Eur. Opt. Soc.-Rapid* **9**, 14020 (2014).
- [5] C. Moore, A. Barnard, P. Fietzek, M. R. Lewis, H. M. Sosik, S. White, and O. Zielinski, "Optical tools for ocean monitoring and research," *Ocean Sci.* **5**, 661–684 (2009).
- [6] G. N. Plass, T. J. Humphreys, and G. W. Kattawar, "Color of the ocean," *Appl. Opt.* **17**, 1432–1446 (1978).
- [7] S. B. Hooker, G. Lazin, G. Zibordi, and S. McLean, "An evaluation of above-and in-water methods for determining water-leaving radiances," *J. Atmos. Oceanic Technol.* **19**, 486–515 (2002).
- [8] J. L. Mueller, G. S. Fargion, C. R. McClain, S. Pegau, J. R. V. Zaneveld, B. G. Mitchel, M. Kahru, et al. (eds.), "Ocean optics protocols for satellite ocean color sensor validation," (NASA, revision 4, 2003).
- [9] S. P. Garaba, and O. Zielinski, "An assessment of water quality monitoring tools in an estuarine system," *Remote Sens. Appl.: Soc. Environ.* **2**, 1–10 (2015).
- [10] E. L. Hestir, V. E. Brando, M. Bresciani, C. Giardino, E. Matta, P. Villa, and A. G. Dekker, "Measuring freshwater aquatic ecosystems: The need for a hyperspectral global mapping satellite mission," *Remote Sens. Environ.* **167**, 181–195 (2015).
- [11] A. Tanaka, H. Sasaki, and J. Ishizaka, "Alternative measuring method for water-leaving radiance using a radiance sensor with a domed cover," *Opt. Express* **14**, 3099–3105 (2006).
- [12] T. Suresh, M. Talaulikar, E. Desa, S. G. Prabhu Matondkar, T. S. Kumar, and A. Lotlikar, "A simple method to minimize orientation effects in a profiling radiometer," *Mar. Geod.* **35**, 441–454 (2012).
- [13] J. Piskozub, "Effect of ship shadow on in-water irradiance measurements," *Oceanologia* **46**, 103–112 (2004).
- [14] R. W. Spinrad, and E. A. Widder, "Ship shadow measurements obtained from a manned submersible," *Proc. SPIE* **1750**, 372–383 (1992).
- [15] K. J. Waters, R. C. Smith, and M. R. Lewis, "Avoiding ship-induced light-field perturbation in the determination of oceanic optical properties," *Oceanography* **3**, 18–21 (1990).
- [16] Hydrographic funnels operator manual, 696 D 0001 (Neptun Werft, 2013).
- [17] I. Reda, and A. Andreas, "Solar position algorithm for solar radiation applications," *Sol. Energy* **76**, 577–589 (2004).
- [18] C. T. Weir, D. A. Siegel, A. F. Michaels, and D. W. Menzies, "In situ evaluation of a ship's shadow," *Proc. SPIE* **2258**, 815–821 (1994).
- [19] S. B. Hooker, and A. Morel, "Platform and environmental effects on above-water determinations of water-leaving radiances," *J. Atmos. Oceanic Technol.* **20**, 187–205 (2003).
- [20] R. Leathers, T. V. Downes, and C. Mobley, "Self-shading correction for upwelling sea-surface radiance measurements made with buoyed instruments," *Opt. Express* **8**, 561–570 (2001).
- [21] C. A. Stedmon, C. L. Osburn, and T. Kragh, "Tracing water mass mixing in the Baltic-North Sea transition zone using the optical properties of coloured dissolved organic matter," *Estuar. Coast. Shelf S.* **87**, 156–162 (2010).
- [22] T. Kristiansen, and E. Aas, "Water type quantification in the Skagerrak, the Kattegat and off the Jutland west coast," *Oceanologia* **57**, 177–195 (2015).